Inorganic Chemistry

pubs.acs.org/IC

Article

Lanthanide Luminescence and Thermochromic Emission from Soft-Atom Donor Dichalcogenoimidodiphosphinate Ligands

Orlando C. Stewart, Jr., Alexander C. Marwitz, Joel Swanson, Jeffery A. Bertke, Tyler Hartman, Jorge H. S. K. Monteiro, Ana de Bettencourt-Dias, Karah E. Knope, and Sarah L. Stoll*

Cite This: *Inorg. Chem.* 2022, 61, 15547−15557

Read Online

ACCESS | Metrics & More | Article Recommendations | Supporting Information

ABSTRACT: The luminescence properties of two divalent europium complexes of the type $Eu[N(SPPh_2)_2]_2(THF)_2$ (**1**) and $Eu[N(SePPh_2)_2]_2(THF)_2$ (**2**) were investigated. The first complex, $Eu[N(SPPh_2)_2]_2(THF)_2$ (**1**), was found to be isomorphous with the reported structure of complex **2** and exhibited room temperature luminescence with thermochromic emission upon cooling. We found the complex $Eu[N(SePPh_2)_2]_2(THF)_2$ (**2**) was also thermochromic but the emission intensity was sensitive to temperature. Both room temperature and low temperature (100 K) single crystal X-ray structural investigation of **1** and **2** indicate geometric distortions of the metal coordination, which may be important for understanding the thermochromic behavior of these complexes. The trivalent europium complex $Eu[N(SPPh_2)_2]_3$ (**3**) with the same ligand as **1** was also structurally characterized as a function of temperature and exhibited temperature-dependent luminescence intensity, with no observable emission at room temperature but intense luminescence at 77 K. Variable temperature Raman spectroscopy was used to determine the onset temperature of luminescence of $Eu[N(SPPh_2)_2]_3$ (**3**), where the 615 nm ($^5D_0 \rightarrow {}^7F_2$ transition) peak was quenched above 130 K. The UV−visible diffuse reflectance of **3** provides evidence of an LMCT band, supporting a mechanism of thermally activated LMCT quenching of Eu(III) emitting states. A series of ten isomorphous, trivalent lanthanide complexes of type $Ln[N(SPPh_2)_2]_3$ (Ln = Eu (**3**) Pr (**4**), Nd (**5**), Sm (**6**), Gd (**7**), Tb (**8**)) and $Ln[N(SePPh_2)_2]_3$ (Ln = Pr (**9**), Nd (**10**, structure was previously reported), Sm (**11**), and Gd (**12**) for Q = Se) were also synthesized and structurally characterized. These complexes for Ln = Pr, Nd, Sm, and Tb exhibited room temperature luminescence. This study provides examples of temperature-dependent luminescence of both Eu^{2+} and Eu^{3+}, and the use of soft-atom donor ligands to sensitize lanthanide luminescence in a range of trivalent lanthanides, spanning near IR and visible emitters.

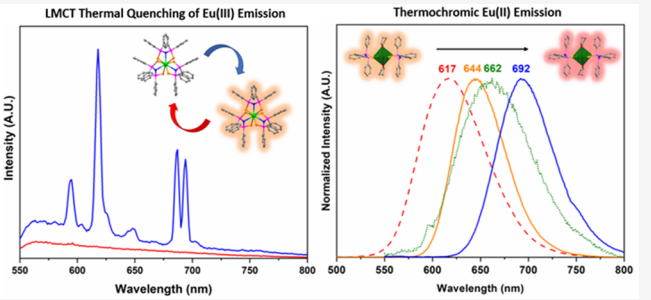

INTRODUCTION

The lanthanides are well-known for their luminescence properties, and europium has held a central interest because it has two oxidations states that can exhibit intense luminescence in the visible part of the spectrum,[1] and into the NIR (for the divalent metal). One of the distinct features of Eu(II) luminescence is the tunable energy emission peak, because the emissive 5d states are sensitive to the ligand environment.[2] In the trivalent state, europium emission typically exhibits red emission with intensity sensitivity to site symmetry.[3] Recently, temperature-dependent luminescence has been of interest for thermo-sensing properties, with demonstrated examples of lanthanide "molecular thermometers".[4] In the case of Eu(III), complexes can undergo ligand-to-metal-charge transfer (LMCT), which leads to thermosensitive luminescence properties.[5,6] The recent discovery of luminescence thermometry in an organometallic Eu(II) complex demonstrates that sensitive "band shift thermometry" is accessible for divalent europium.[7] Here, we have identified three more examples of temperature-dependent luminescence in both Eu(II) and Eu(III) systems, as well as room temperature emission in Pr, Nd, Sm, and Tb.

Our interest in single-source precursors for lanthanide chalcogenide nanomaterials (e.g., dithiocarbamate chelates to form EuS,[8] and diselenophosphinate complexes to form $LnSe_2$, Ln = lanthanide)[9] led us to investigate the lanthanide complexes of the dichalcogenoimidodiphosphinates, $[N(QPR_2)_2]^-$ (R = alkyl, aryl, Q = S, Se). This ligand system provides the widest soft-atom donor comparison because it is known to stabilize the full range of Q from O to Te and is able to stabilize the divalent lanthanides Eu and Sm.[10−12] Transition metal dichalcogenoimidodiphosphinates complexes have found application as single-source precursors for chemical

Received: June 30, 2022
Published: September 16, 2022

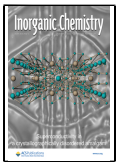

https://doi.org/10.1021/acs.inorgchem.2c02260
Inorg. Chem. 2022, 61, 15547−15557

vapor deposition[13,14] and nanoparticle synthesis.[15−17] Recently, there has also been growing interest in lanthanide and actinide dichalcogenoimidodiphosphinate complexes as model systems for investigating differences in covalency between 4f and 5f elements, to enhance a fundamental understanding of bonding in these metals.[18,19] Differences in soft-donor coordination chemistry may also be an important aid in lanthanide and actinide separations.[20]

Lanthanide complexes with the oxo- version, $[N(OPR_2)_2]^-$, have previously been investigated as antenna ligands for lanthanide luminescence,[21] with the advantage of forming a "hydrophobic shield" to enhance lanthanide luminescence.[22] The ligand is not only strongly absorbing, but the shell prevents solvent deactivation routes.[23,24] Moreover, studies on the effects of fluorination and methylation of these complexes have observed electronic effects on the emissive properties of lanthanides, adding considerations for the development of advanced luminescent materials.[25] Although these ligands are a good model for investigating donor ligand electronic effects on lanthanide luminescence, reports have been limited to the O-containing analogs, providing an opportunity to investigate soft-atom donor ligands for lanthanide luminescence.

Based on the emissive properties of the lanthanide dithiocarbamates,[26] and the success of the dioxo-imidodiphosphinates, we investigated the luminescence of the lanthanide dichalcogenoimidodiphosphinate complexes. Interest in soft donors for luminescent complexes in part has been driven by the observation that the low phonon energy of the Ln−Q bonds avoids deactivation of efficient NIR luminescence.[27] Evidence that the soft donors are capable of sensitization can be found in other ligand classes, such as the dithiophosphinates.[28] Examples include $Sm(Q_2PPh_2)_3(THF)_2$, for Q = S, Se,[27] and tetra-kis $(Et_4N)[Ln(S_2P(CH_2CH_2Ph)_2)_4]$, for Ln = Sm, Eu, and Tb.[29] There are several other mixed-ligand examples; however, there is some ambiguity confirming sensitization given that complexes such as $Ln(phen)L_3$ and $Ln(phen)L_2(NO_3)$ contain phenanthroline, a well-studied antenna ligand.[30] Because aromatic groups in the antenna are thought to improve the luminescence of Ln(III) complexes, we targeted the $[N(QPR_2)_2]^-$ where R = phenyl.[29] In addition to divalent and trivalent europium emission, we sought to synthesize a wider series of trivalent lanthanide complexes utilizing the phenyl substituted dithio- and diselenoimidodiphosphinate ligands to probe their photophysical properties.

Here, we report the synthesis and single-crystal structures of three europium-based complexes, $Eu[N(SPPh_2)_2]_2(THF)_2$ (**1**), the previously reported $Eu[N(SePPh_2)_2]_2(THF)_2$ (**2**),[19] and $Eu[N(SPPh_2)_2]_3$ (**3**). Using the same sulfur and selenium ligands, complexes were also prepared with a range of lanthanides and single-crystal structures of the corresponding isomorphous compounds: $Ln[N(SPPh_2)_2]_3$ (Ln = Pr (**4**), Nd (**5**), Sm (**6**), Gd (**7**), Tb (**8**)) and $Ln[N(SePPh_2)_2]_3$ (Ln = Pr (**9**), Sm (**11**), Gd (**12**)) are presented. The crystal structure of $Nd[N(SePPh_2)_2]_3$ (**10**) has been previously reported[19] (and related actinide complex $Np[N(SePPh_2)_2]_3$);[31] here, we investigate its photophysical properties. The divalent europium complexes $Eu[N(SPPh_2)_2]_2(THF)_2$ (**1**) and $Eu[N(SePPh_2)_2]_2(THF)_2$ (**2**) both exhibit thermochromic emission, and **1** has intense luminescence at room temperature. Unexpectedly, compared with other bright emitters, the trivalent europium complex (**3**) is not emissive at room temperature but cooling leads to increased luminescence intensity and its emission is visually intense at 77 K. To assess structural changes of $Eu[N(SPPh_2)_2]_3$ (**3**) with temperature, we used variable-temperature single crystal X-ray diffraction, but did not observe significant symmetry changes, just the expected bond length contraction as the compound cooled (see S17). Using variable-temperature Raman spectroscopy to monitor the luminescence of complex **3**, we determined the temperature at which emission is quenched. Spectroscopic studies of the trivalent complexes show that these ligands are able to sensitize Ln^{3+} emission. These studies suggest that the dichalcoimidodiphosphinate ligands provide a new example of soft-atom donor ligand sensitization and, surprisingly, the ability to form luminescent complexes for both Eu(II) and Eu(III).

EXPERIMENTAL SECTION

Materials. All starting materials purchased commercially were used as received with no further purification. Lanthanide(III) bis(trimethylsilyl)amide salts, $Ln[N(SiMe_3)_2]_3$ (where Ln = Sm and Gd), were purchased from Sigma-Aldrich. Tris[N,N-bis-(trimethylsilyl)amide] neodymium(III), 98% was purchased from Fisher Scientific. Lanthanide(III) trifluoromethanesulfonate salts, $Ln(OTf)_3$ (where Ln = Pr and Dy; 98%), were purchased from Alfa Aesar. Europium(III) trifluoromethanesulfonate, 98% was purchased from Fisher Scientific, and terbium(III) trifluoromethanesulfonate, 98% was purchased from Sigma-Aldrich. Potassium bis(trimethylsilyl)amide, 95% and anhydrous europium(II) iodide, 99.9% were purchased from Sigma-Aldrich. *N,N*-Bis(diphenylphosphino)amine ≥98% was purchased from Strem Chemicals. Elemental sulfur and selenium were purchased from Sigma-Aldrich. Anhydrous hexanes (Sigma-Aldrich), anhydrous toluene (Sigma-Aldrich), and anhydrous tetrahydrofuran (Sigma-Aldrich) were used as received.

Synthetic Methods. *Synthesis of $Ln[N(SiMe_3)_2]_3$.* The lanthanide bis(trimethylsilyl)amide salts that could not be purchased commercially (i.e., Pr, Tb, and Dy) were prepared using previously reported methods.[45] Briefly, the amide salts were obtained by refluxing lanthanide trifluoromethanesulfonate salts with potassium bis-(trimethylsilyl)amide in boiling toluene overnight. The resulting solution was pumped dry *in vacuo*, and the resulting products dissolved in toluene and were filtered through Celite. The resulting solutions were pumped dry once more, and the product was used as synthesized.

Synthesis of $NH(QPPh_2)_2$ (Q = S or Se). The ligand, $NH(QPPh_2)_2$, was prepared using previously reported methods by reacting $NH(PPh_2)_2$ with elemental sulfur or selenium in boiling toluene.[46,47] Upon cooling, white crystals precipitated out of solution and were isolated and dried *in vacuo*. The resulting products were recrystallized in hot toluene and used as synthesized. The FTIR spectra of the ligands are included in S6 and S7.

Synthesis of $Eu[N(QPPh_2)_2]_2(THF)_2$ (Q = S, Se). The divalent complexes (**1**−**2**) were prepared via two routes as described in detail in S1. Complex **1** was prepared directly from EuI_2 and $NH(SPPh_2)_2$ in THF, while complex **2** was prepared by treating 1 equiv of $Eu[N(SiMe_3)_2]_3$ with 3 equiv of $NH(SePPh_2)_2$ in THF as previously reported,[19] and through the more direct route of using EuI_2 and $NH(SePPh_2)_2$ in THF. The synthetic details and elemental analysis can be found in Supporting Information S1, as well as the powder diffraction patterns (S2) and FTIR spectrum (S5).

Synthesis of Lanthanide$[N(QPPh_2)_2]_3$ (Q = S, Se). The trivalent lanthanide complexes (**3**−**12**) were prepared by modifying a previously reported protonolysis reaction between the appropriate lanthanide bis(trimethylsilyl)amide, $Ln[N(SiMe_3)_2]_3$, and $NH(QPPh_2)_2$, (where Q = S or Se).[1] Complete synthetic details and elemental analysis can be found in the Supporting Information (S1), as well as the powder diffraction patterns (S2) and FTIR spectra (S6, S7).

https://doi.org/10.1021/acs.inorgchem.2c02260
Inorg. Chem. 2022, 61, 15547−15557

Characterization. Elemental analysis (C, H, N) was performed on a PerkinElmer 2400 microanalyzer using acetanilide as a standard. Powder X-ray diffraction patterns were collected to confirm purity and check for possible polymorphs using a Rigaku Ultima IV X-ray powder diffractometer with Cu Kα radiation at 40 kV and 30 mA and a D/teX silicon strip detector. FTIR measurements were recorded in the range 400−4000 cm^{-1}, from pressed pellets in KBr on a PerkinElmer FTIR instrument. Variable Temperature Raman spectroscopy was performed with a Horiba Raman microscope equipped with 405 and 532 nm lasers and an 1800 line/mm grating and calibrated against a diamond standard. The instrument was interfaced with an Olympus BH2-UMA optical microscope, and a magnification factor of 50× SLWD was used. Spectra were recorded in extended scan mode from 200 to 3000 cm^{-1} and analyzed using the WiRE 2.0 software package. The temperature was controlled using a Linkam FTIR600 temperature stage. Diffuse reflectance measurements were collected on an Agilent Cary 5000 UV−vis−NIR spectrophotometer. Samples were ground into powders and diluted with MgO. The instrument was run in internal diffuse reflectance mode and absorbance measured from 200 to 800 nm. For complex **3**, diffuse reflectance data were also collected using an OceanOptics DH-2000-BAL light source with a fiber-optic probe.

X-ray Crystallography. Single crystals of compounds **1** (100 K), **3** (100 K) **4**−**9**, **11**−**12** were mounted under mineral oil on an MiTeGen Micromount and immediately placed in a cold nitrogen stream at 100(2) K prior to data collection. Compounds **1** (298 K), **2** (298 K), and **3** (298 K) were placed in a nitrogen stream at 298(2) K prior to data collection. Data for compounds **1** (100 K), **1** (298 K), **2** (298 K), **4**, **5**, **6**, **8**, and **9** were collected on a Bruker D8 Quest equipped with a Photon100 CMOS detector and a Mo IμS source. Data for compounds **3** (100 K), **3** (298 K), **7**, **11**, **12**, and **13** were collected on a Bruker APEX DUO equipped with an ApexII detector and a Mo Kα fine-focus sealed tube source. A series of phi and omega scans were collected (Mo Kα radiation, λ = 0.7107 Å) and integrated with the Bruker SAINT program. Structure solutions were performed using the SHELXTL software suite. Intensities were corrected for Lorentz and polarization effects, and an empirical absorption correction was applied using SADABS v2014/4. Non-hydrogen atoms were refined with anisotropic thermal parameters, and hydrogen atoms were included in idealized positions unless otherwise noted. For structures **3** (100 K), **3** (298 K), **4**, **5**, **6**, **7**, **8**, **9**, **11**, and **12**, the disordered toluene was modeled so the ring carbon (C13) is 100% occupied and the methyl (C14) is 1/6 occupied. The H atom on C13 is 5/6 occupied, so the solvent formula comes to C_7H_8 as expected. Additionally, the C13−C14 was restrained to be 1.50 (esd 0.01). In the structure of **1**−**100**, two phenyl rings are disordered over two orientations. The like P−C and C−C distances were restrained to be similar. Additionally, the THF molecule is disordered over two orientations. The like O−C and C−C distances were restrained to be similar. The O1/O1B and C19/C19B atom pairs were constrained to have equal *x*, *y*, *z* positions and equal anisotropic displacement parameters. Similar displacement amplitudes were imposed on disordered sites overlapping by less than the sum of van der Waals radii. In the structure of **1** (298 K), two phenyl rings are disordered over two orientations. The like P−C and C−C distances were restrained to be similar. Additionally, the THF molecule is disordered over two orientations. The like O−C and C−C distances were restrained to be similar. The O1/O1B, C13/C13B, and C19/C19B atom pairs were constrained to have equal *x*, *y*, *z* positions and equal anisotropic displacement parameters. Similar displacement amplitudes were imposed on disordered sites overlapping by less than the sum of van der Waals radii. Complete crystallographic details for each complex are provided in the Supporting Information.

*Photophysical Characterization for Complexes **1**−**4**, **7**−**9**, and **12**.* Excitation and emission spectra were collected using a Horiba PTI QM-400 spectrofluorometer equipped with a Xe light source. Solid samples of measured complexes were ground and pressed between two quartz microscope slides for collection, except for complexes **1**−**3**, **7**, and **12**, which were placed in NMR tubes for room temperature and low temperature collections. Low temperature excitation and emission spectra were collected by immersing the sample in liquid nitrogen at 77 K using a Cold Finger Dewar K-158 attachment. When necessary, a 400 nm long pass filter was used to avoid harmonic peaks from the excitation source and slit widths for all measurements ranged from 3 to 5 nm. All emission and excitation spectra were corrected. Lifetime measurements were collected with a lamp frequency of 100 Hz. Results were plotted in OriginPro 8.5 and fit with exponential decay curves, generating decay functions and fitting parameters for each sample. These can be found in the Supporting Information (S9−S12). Triplet states for the ligands were determined by using a frozen glass matrix of a solution consisting of $Gd[N(SiMe_3)_2]_3$ and the corresponding ligand dissolved in THF. Time-resolved emission spectra were collected with 5 nm spectral widths using a 1000−2000 μs collection window after excitation to remove residual fluorescence, leaving only phosphorescence from the ligands. Triplet state energies were then determined from the onset of emission, for the gadolinium complexes (**7**, **12**), and these data can be found in the Supporting Information (S8).

*Photophysical Characterization for Complexes **5**−**6** and **10**−**11**.* Solid-state samples were used to obtain the emission and excitation spectra. The photoluminescence data were obtained on an Edinburgh FS5 spectrofluorometer, with an excitation monochromator with 1200 grooves/mm and gratings blazed at 330 nm and an emission monochromator with 1200 grooves/mm and gratings blazed at 500 nm. An ozone-free 150 W xenon lamp (Ushio) was used as a radiation source. The excitation spectra, corrected for instrumental function, were measured between 250 and 500 nm. The emission spectra were measured in the range 500−750 nm using a Hamamatsu 928P detector. All emission spectra were corrected for instrumental function. The emission decay curves were obtained using a TCSPC system and a Xe pulsed lamp as an excitation source. The NIR photoluminescence data for complexes **5** and **10** were obtained on a Fluorolog-3 spectrofluorometer (Horiba FL3−22-iHR550), with an excitation monochromator with 1200 grooves/mm and gratings blazed at 330 nm and an emission monochromator with 1200 grooves/mm and gratings blazed at 500 nm. An ozone-free 450 W xenon lamp (Ushio) was used as a radiation source. The excitation spectra, corrected for instrumental function, were measured between 250 and 600 nm. The emission spectra were measured in the range 800−1425 nm using a Hamamatsu 5509-73 detector cooled with liquid N_2. All emission spectra were corrected for instrumental function.

RESULTS AND DISCUSSION

Synthesis. The divalent europium complexes, $Eu[N(SPPh_2)_2]_2(THF)_2$ (**1**) and $Eu[N(SePPh_2)_2]_2(THF)_2$ (**2**), were prepared using a similar route as reported for the samarium complexes $Sm[N(QPPh_2)_2]_2(THF)_2$ for Q = S, Se,[32] by reacting a divalent lanthanide halide (e.g., EuI_2) with the ligand. Interestingly, the divalent europium analog, $Eu[N(SePPh_2)_2]_2(THF)_2$ (**2**), forms when attempting to prepare the trivalent complex from 3 equiv of $NH(SePPh_2)_2$ with $Eu[N(SiMe_3)_2]_3$.[19] The unsuccessful synthesis of the complex with Eu(III) and the selenium ligand is due to the favored ligand reduction chemistry forming Eu(II) at room temperature, unlike the sulfur version.[19] This is consistent with calculations of electronic populations of similar complexes such as $La[N(QP^iPr_2)_2]_3$ for Q = O, S, Se, and Te, which indicate a decrease in the lanthanum charge from oxygen to tellurium. This is also supported by the ability to form $Eu^{3+}[N(QPPh_2)_2]_3$ for Q = O and S, but Q = Se leads to the divalent europium complex (there are no reports of the Te complex).[33] The ligand reduction chemistry is one of the methods for preparing divalent europium complexes,[34] and in nanoparticle synthesis of EuS, the dithiocarbamate ligand has been found to reduce Eu(III) to Eu(II), however at much higher temperatures.[35] The reducing ability of the selenium

https://doi.org/10.1021/acs.inorgchem.2c02260
Inorg. Chem. 2022, 61, 15547−15557

ligand is promising for the synthesis of divalent europium monoselenide nanoparticles.

The trivalent lanthanide complexes reported here were all prepared by reacting the highly soluble trimethylsilylamide salt of the lanthanide ($Ln[N(SiMe_3)_2]_3$) in toluene with $NH(SPPh_2)_2$ or $NH(SePPh_2)_2$ in THF (tetrahydrofuran). Successful deprotonation of the ligand leads to complex formation and crystallization of $Ln[N(QPPh_2)_2]_3$ upon layering of the two reactant solutions. This route proved successful at growing X-ray quality crystals, so we did not optimize the synthesis further. The solubility of the complexes was quite low in most organic solvents, and the more soluble complexes decolorized over time, so the spectroscopic studies here were of solid-state crystals. By contrast, the previously reported oxygen analogs form complexes, $Ln[N(OPPh_2)_2]_3(EtOH)$ (thus 7-coordinate), for Ln = Tb, Eu, Dy, Gd, and Er, and exhibited high solubility and solution stability in a range of solvents.[36] It is worth noting that the selenium complex with the smallest lanthanide reported here, $Tb[N(SePPh_2)_2]_3$, did not crystallize and drying the solution *in vacuo* led to ligand crystallization.

Structural Description. The single crystal structure for three divalent lanthanide complexes with the dichalcogenoimidodiphosphinate ligands have recently been reported, including $Eu[N(SePPh_2)_2]_2(THF)_2$ (**2**),[19] as well as $Sm[N(QPPh_2)_2]_2(THF)_2$ Q = S, Se.[32] Here we report the bis europium complex, $Eu[N(SPPh_2)_2]_2(THF)_2$ (**1**), in which the ligands are bidentate as observed for complex **2**. As shown in Figure 1, even with two solvent molecules in the coordination

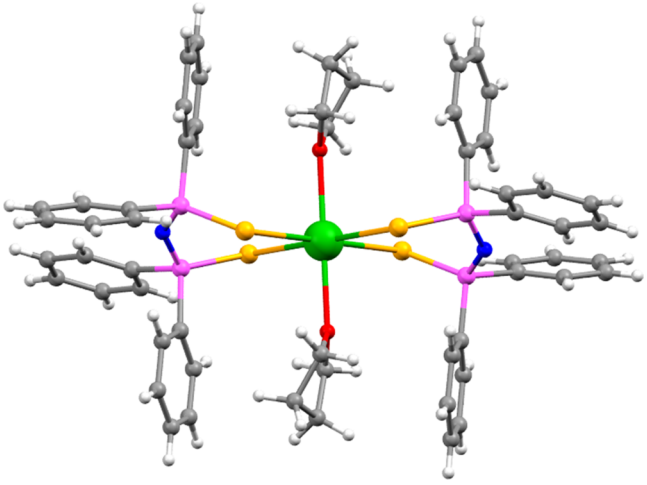

Figure 1. Structure of $Eu[N(SPPh_2)_2]_2(THF)_2$ (**1**) which is isomorphous with $Eu[N(SePPh_2)_2]_2(THF)_2$ (**2**). The Eu is shown in green, C in gray, O in red, P in purple, N in blue, and Se in orange.

sphere, the coordination number 6 is low for a lanthanide. There are examples of low coordinate divalent lanthanides including planar 4-coordinate Yb(II) and Sm(II); however, these are typically for sterically bulky ligands.[37,38] Interestingly, in both complex **1** and **2**, nonequivalent Eu−Q bond lengths are present, showing the flexibility of these ligands when bound in a bidentate fashion. In complex **1**, Eu−S bond lengths of 2.91 and 2.94 Å are observed, while Eu−Se bond lengths of 3.08 and 3.11 Å are present. As discussed later, coordination of these ligands in a tridentate-fashion results in equivalent Ln−Q bond lengths for the trivalent lanthanides, including Eu.

Several trivalent lanthanide complexes with the dichalcogenoimidodiphosphinate ligand have also been reported. The single crystal structures were reported for both sulfur and selenium analogs with the largest lanthanides: $Ln[N(QPPh_2)_2]_3$ for Ln = La and Ce (Q = S, Se),[39] as well as the selenium analog for $Nd[N(SePPh_2)_2]_3$ (**10**).[19] The structures determined here include $Ln[N(SPPh_2)_2]_3$, for Ln = Eu (**3**), Pr (**4**), Nd (**5**), Sm (**6**), Gd (**7**), Tb (**8**), and $Ln[N(SePPh_2)_2]_3$, for Ln = Pr (**9**), Sm (**11**), and Gd (**12**). These complexes, shown in Figure 2, are homoleptic and

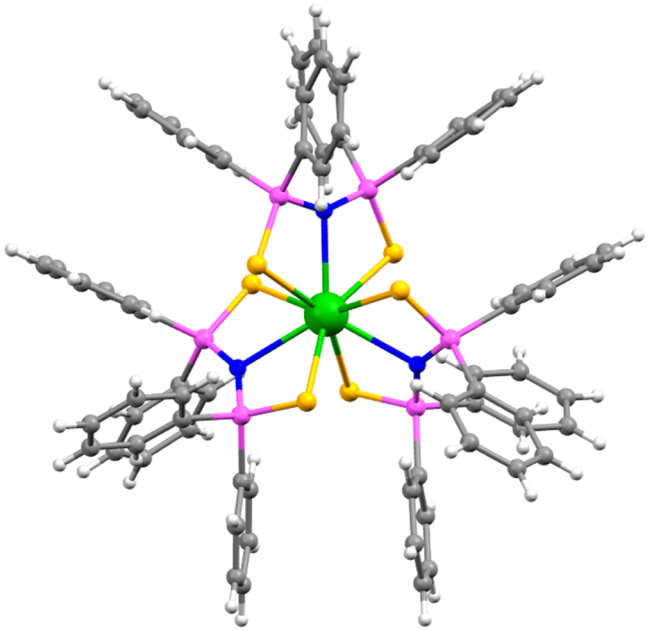

Figure 2. Representative structure of $Ln[N(SPPh_2)_2]_3$ (Ln = Eu (**3**), Pr (**4**), Nd, (**5**) Sm (**6**), Gd (**7**), Tb (**8**)) and $Ln[N(SePPh_2)_2]_3$ (Ln = Pr (**9**), Nd (**10**, previously reported), Sm (**11**), Gd (**12**) Q = Se). The Ln is shown in green, C in gray, P in purple, N in blue, and S or Se in orange.

isomorphous to those reported previously. The compounds crystallize in $R\bar{3}c$, with the metal center exhibiting D_3 symmetry. The central lanthanide in these complexes is nine-coordinate due to the tridentate nature of the ligand (bonding through the chalcogen and the central nitrogen).

One benefit of having an isomorphous series is the comparison of lanthanide−nitrogen and lanthanide−chalcogen bond lengths across the series. The tris complexes have tridentate $N(QPPh_2)_2^-$ where the Ln−N bond distances 2.65−2.55 Å are shorter for Q = S, than Q = Se (see Supporting Information S19). When comparing Ln−Q bond distances, evidence of the lanthanide contraction is observed, with the Ln−S bond lengths ranging between 3.02 and 2.92 Å, and longer Ln−Se bond lengths ranging from 3.12 to 3.04 Å. Interestingly, the gradual and consistent decrease in Ln−S bond lengths deviates for Eu, which has a longer bond length than expected (see S19). In fact, the Eu−S bond length in complex **3** (2.95 Å) is similar to those observed in the divalent complex **1** (2.91 and 2.94 Å). This highlights the electron donating ability of these soft chalcogen-containing ligands and the lower reduction potential for europium. Previous theoretical work on Eu complexes with these ligands found that europium can exhibit 'Eu^{2+}-like behavior',[33] predicting a

https://doi.org/10.1021/acs.inorgchem.2c02260
Inorg. Chem. 2022, 61, 15547−15557

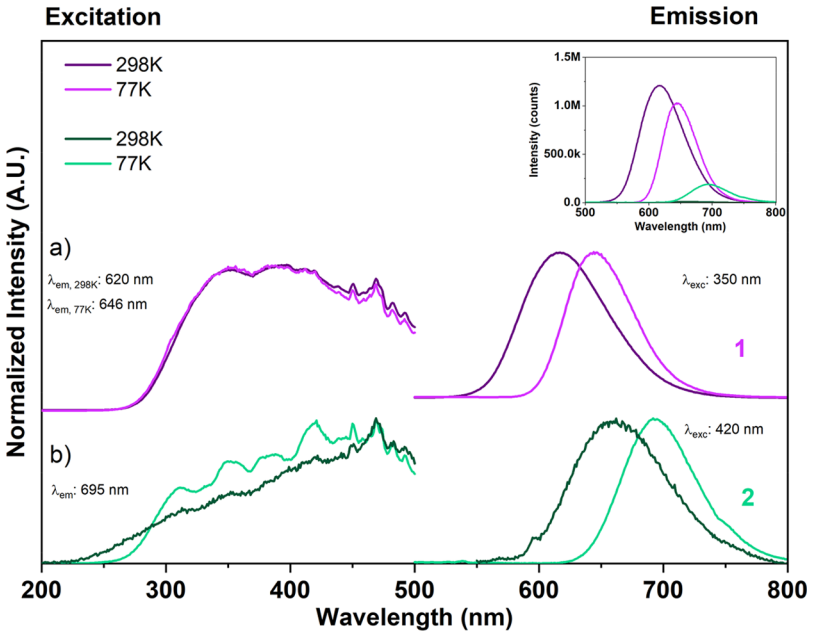

Figure 3. Normalized RT and 77 K excitation and emission spectra of (a) $Eu[N(SPPh_2)_2]_2(THF)_2$ (**1**) and (b) $Eu[N(SePPh_2)_2]_2(THF)_2$ (**2**). Inset shows relative emission intensities of complexes **1** and **2** at rt and 77 K. Complex **1** exhibits strong luminescence at RT and 77 K, while complex **2** only exhibits significant emission intensity at 77 K.

long Eu−S bond length. Our experimentally determined Eu−S bond length (2.95 Å) supports this.

What is interesting is not only the constant denticity across the $Ln[N(QPPh_2)_2]_3$ series of complexes for both Q = sulfur and selenium but also the symmetry around the metal, and the space group remained unchanged. This is distinctly different from the $Ln[N(OPPh_2)_2]_3$ complexes, in which there are examples (such as Tb, Eu) where there is more than one molecule per unit cell with different symmetries around the metal,[21] or other examples (such as Nd) in which several polymorphs can form.[19] To confirm that the single crystals are representative of the bulk product, we have included the powder diffraction pattern of all complexes in the Supporting Information (S2, S3) and compared them to the calculated powder patterns from the cif of the single crystal structures.

The bonding geometry and ligand covalency are important parameters with effects on the optical properties of lanthanide complexes. Symmetry, even subtle shifts around the metal, can alter the luminescence.[40] One of the interesting features of the dichalcogenoimidodiphosphinate is the variable denticity of the $N(QPR_2)_2^-$ (Q = O, S, Se, Te) ligand; it can be bidentate κ^2 (Q, Q) or tridentate κ^3 (QNQ, i.e., through donation from the nitrogen). The denticity appears to be determined in the balance of several factors: the metal, the donor chalcogen (Q), and the R group on phosphorus. Compared to the smaller transition metal complexes which all have bidentate coordination, we see tridentate coordination of $N(QPPh_2)_2^-$ (Q = S, Se) for the trivalent lanthanides, suggesting that metal radii might be important. However, ionic radii are not determinative, as the divalent lanthanides which have larger ionic radii than the trivalent lanthanides form bidentate complexes for $Ln[N(SPPh_2)_2]_2(THF)_2$ (Ln = Eu and Sm) and $Eu[N(SePPh_2)_2]_2(THF)_2$. Interestingly, the selenium analog for Sm(II), $Sm[N(SePPh_2)_2]_2(THF)_2$, is split, with one bidentate ligand and one tridentate suggesting these are very close in stability. The identity of Q may also be important, as in the trivalent lanthanides in $Ln[N(OPPh_2)_2]_3$, where the donor atom (Q) is oxygen, the ligand is bidentate,[25] unlike S, and Se with the same metal. The final factor determining denticity, the nature of the R group, is also important. For example, in the lanthanum complex, $La[N(QPR_2)_2]_3$ for all Q = S, Se and R = phenyl, the ligand is bidentate, whereas, for R = ^{i}Pr, the ligand is tridentate.[39] This has been ascribed to a steric effect, due to the increased bulk of the ^{i}Pr compared to phenyl rings. The tellurium analog has some ambiguity, as the ligand with R = Ph is difficult to synthesize, and most metal complexes have been prepared with the R = ^{i}Pr which is more electron donating, stabilizing the P═Te bond.[41]

Vibrational Spectroscopy. FTIR was utilized to confirm successful complex formation by changes to the spectra upon deprotonation and coordination to the metal. Spectra collected for the free ligand and compared to the complexes are shown in the Supporting Information (S5−S7). The free $N(SPPh_2)_2^-$ ligand showed a δ(N−H) bending mode around 1326 cm^{-1} that is absent in the spectra of the trivalent complexes, confirming successful deprotonation of the ligand backbone. The same deprotonation is observed for the Se-analogs, as the δ(N−H) bend around 1323 cm^{-1} in the free $N(SePPh_2)_2^-$ ligand is absent in the complexes. We also observe strong vibrations located at ∼595 cm^{-1} for complexes **3**−**8**, and ∼593 cm^{-1} for complexes **9**−**12**, that we attribute to the ν(P−Q) vibrations, based on previously reported assignments for isomorphous complexes.[42] Additionally, the ν(P−N−P) vibration located around 785 cm^{-1} in the $N(SPPh_2)_2^-$ and 765 cm^{-1} in the $N(SePPh_2)_2^-$ free ligands is absent when the ligand complexes the metal in a tridentate fashion. Interestingly, in the divalent complexes this vibration shifts in energy (783 cm^{-1} in complex **1** and 770 cm^{-1} in complex **2**), consistent with the bidentate coordination mode of the ligand.

Room Temperature and Thermochromic Luminescence of $Eu[N(SPPh_2)_2]_2(THF)_2$ (1). The luminescence in Eu(II) differs from Eu(III) because the low lying 5d states lead to strong 5d → 4f emission. Because of the sensitivity of the 5d orbitals to the ligand donors, this emission is very sensitive to

https://doi.org/10.1021/acs.inorgchem.2c02260
Inorg. Chem. 2022, 61, 15547−15557

the environment and, thus, highly tunable.[43] We also observe that both divalent europium complexes ($Eu[N(QPPh_2)_2]_2(THF)_2$ Q = S, Se) exhibit a strong thermochromic shift (as shown in Figure 3). The first thermally sensitive luminescent Eu(II) complex was reported recently for $[Cp^*Eu(\mu\text{-}BH_4)(THF)_2]_2$, with luminescence that shifted over a broad temperature range (60−320 K).[7] With increasing temperature, the emission wavelength blue-shifted from 19 501 to 20 769 cm^{-1} (difference of 1268 cm^{-1}). The blue shift was explained by considering the changes in metal−ligand bonds which increase with temperature leading to smaller ligand field effects at high temperatures (smaller splitting leads to a larger 4f to 5d energy gap), as illustrated in Figure 4a. The metal−

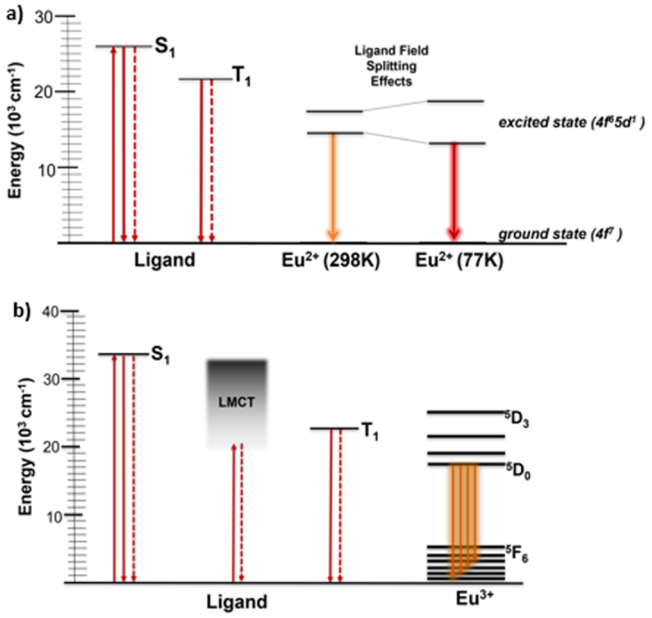

Figure 4. Generalized energy level diagrams for (a) complexes **1** and **2**, (b) complex **3**. In (a), ligand field splitting effects due to differences in metal−ligand bond lengths as a function of temperature result in variation of the Eu^{2+} excited state energy, thus tuning the emission color with temperature. In (b), the LMCT band rests in a location that either overlaps or is very close to the S1, T1, and $^5D_0$ excited state of Eu^{3+} suggesting several nonradiative deactivation pathways to quench Eu^{3+} emission.

ligand covalency tends to increase with increasing polarizability of the ligand, so it is not surprising that the room temperature emission of these complexes, $Eu[N(QPPh_2)_2]_2(THF)_2$ (617 nm for Q = S, and 662 nm for Q = Se), is much lower in energy than $[Cp^*Eu(\mu\text{-}BH_4)(THF)_2]_2$ (483 nm). Here, the sulfur analog, $Eu[N(SPPh_2)_2]_2(THF)_2$, exhibits a blue shift from 644 nm at 77 K to 617 nm at room temperature (or 15 528 cm^{-1} to 16 207 cm^{-1}, ΔE = 679 cm^{-1}). The thermochromic properties for the divalent complex are thought to be due to structural changes with temperature because of the known sensitivity of Eu(II) to geometry, ligand donation, and polarizability. A comparison of high (298 K) and low (100 K) temperature structures determined via single crystal X-ray diffraction, as illustrated in Figure 5, confirm shifts in the bond lengths as well as distortions in the coordination octahedron as the temperature is decreased. Although the site symmetry of the metal is unchanged and the changes in bond length are not large (~0.05 Å), the effect is notable because the ligands are aligned toward the d orbitals.

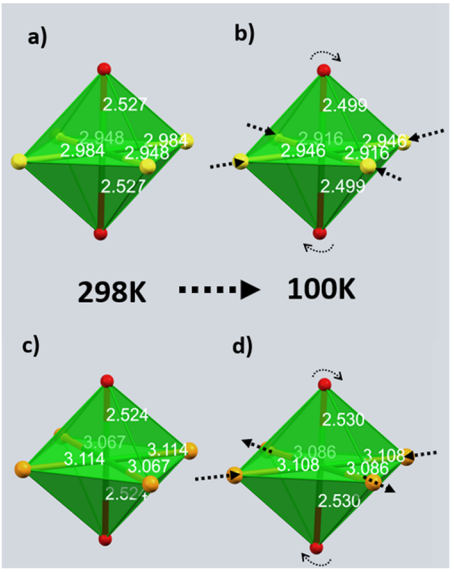

Figure 5. Distortion of Eu(II) coordination environment in $Eu[N(SPPh_2)_2]_2(THF)_2$ (**1**) and $Eu[N(SePPh_2)_2]_2(THF)_2$ (**2**) as a function of temperature. Bond lengths are shown in white for (a) **1** at 298 K, (b) **1** at 100 K, (c) **2** at 298 K, and (d) **2** at 100 K.[19]

Thermochromic Luminescence of $Eu[N(SePPh_2)_2]_2(THF)_2$ (2). Europium is differentiated from the rest of the lanthanides because of the far lower EuIII/II redox potential (−0.35 V) and stability of the divalent metal particularly in the presence of the soft chalcogen donor. The inability to stabilize the trivalent $Eu[N(SePPh_2)_2]_3$ compound, and formation of divalent $Eu[N(SePPh_2)_2]_2(THF)_2$, is consistent with the ability of the ligand to reduce europium, and a matching of the soft Eu(II) with a soft Se donor, in the Hard−Soft-Acid−Base (HSAB) sense. Interestingly, this complex also exhibits temperature-dependent luminescence (Figure 3b). Similar to complex **1**, significant blue-shifting of the emission peak was observed in complex **2** with increased temperature. The room temperature emission of **2**, $Eu[N(SePPh_2)_2]_2(THF)_2$, at 692 nm (14451 cm^{-1}) is even lower in energy than the emission of **1**, $Eu[N(SPPh_2)_2]_2(THF)_2$, due to the softer nature of Se compared with S. Moreover, unlike complex **1**, which exhibited intense luminescence at RT and 77 K, complex **2** exhibits very weak luminescence at RT (inset to Figure 3). Upon cooling to 77 K, emission was observed at 662 nm (the shift in energy was 655 cm^{-1}, similar in magnitude to the sulfur analog). As described for the sulfur analog, the variable-temperature single crystal X-ray diffraction indicates strong distortions of the coordination polyhedron and changes in bond length with temperature.

Temperature Dependent Luminescence and Thermochromism in $Eu[N(SPPh_2)_2]_3$ (3). Trivalent europium complexes typically exhibit a maximum quantum yield when the triplet state of the ligand is between the $^5D_2$ and $^5D_1$ levels of Eu(III), in the range 21 500−22 500 cm^{-1}.[44] To estimate the triplet energy levels, we used the common method of comparing the analogous chelates of a nonemitting lanthanide, Gd^{3+}. As shown in the Supporting Information (S8), the phosphorescence spectra of the $Gd[N(SPPh_2)_2]_3$ complex correspond to a ^3T energy of 22 730 cm^{-1} (440 nm), while the selenium analog, $Gd[N(SePPh_2)_2]_3$, corresponds to a ^3T energy of 21 740 cm^{-1} (460 nm). The dithio-imidodiphosphinate ligand ($[N(SPPh_2)_2]$) has a triplet energy only slightly

https://doi.org/10.1021/acs.inorgchem.2c02260
Inorg. Chem. 2022, 61, 15547−15557

lower in energy from that of the dithiocarbamate ligand, 23 095 cm^{-1}. Thus, one would expect emission from both the tris thio- and seleno-imidodiphophinate (which we were unable to prepare). However, the trivalent europium complex, $Eu[N(SPPh_2)_2]_3$, is not luminescent at room temperature; rather, the emission is intense at 77 K, as shown in Figure 6. One possibility for the quenching effect is photoinduced electron transfer,[45] which would not be surprising given the reduction of europium in the presence of the selenium analog.

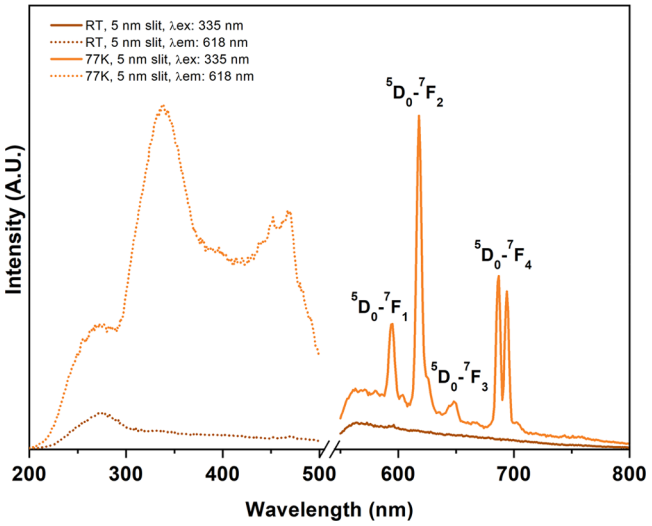

Figure 6. Excitation and emission spectra of $Eu[N(SPPh_2)_2]_3$ (**3**) at RT and 77 K.

We believe the temperature dependence can be ascribed to the presence of ligand-to-metal charge transfer (LMCT) quenching.[6] The europium dithiocarbamate complexes also exhibit LMCT quenching of the emission at room temperature,[46] and many other chelates have been reported to display this mechanism.[6] The trivalent complex $Eu[N(SPPh_2)_2]_3$, (**3**), as can be seen in Figure 6, has broad excitation bands at 77 K that are not apparent at room temperature and suggest, as observed for the europium dithiocarbamate, that the population of the 4f states is quenched at room temperature by the LMCT states. The efficient ligand-to-metal charge transfer process is supported by the broad ligand-centered absorption band in the UV−visible diffuse reflectance spectra (Figure 7), centered at 408 nm. We calculate the LMCT energy from the onset rise absorption at the low energy side of the peak (17 543 cm^{-1}), which is lower than that reported for the $Eu(S_2CNR_2)_3$phen (R = Et = 19 080 cm^{-1} and R = Ph = 19 960 cm^{-1}).[46] As shown in the energy level diagram in Figure 4b, the LMCT band falls very close to the emissive excited states of Eu(III) and overlaps with the triplet state of the ligand. This suggests various energy transfer processes (i.e., depopulation of S_1 to LMCT, back-energy transfer from T to LMCT, and back-energy transfer from Eu(III) to LMCT) that can depopulate the europium excited states, quenching luminescence. Although the LMCT transition probability depends on the coordination geometry, the mixing of the 4f and p-orbitals is also very sensitive to M−L distance. The low temperature luminescence has a higher intensity band for the $^5D_0 \rightarrow {}^7F_2$ transition than the $^5D_0 \rightarrow {}^7F_1$, indicating low symmetry around the Eu(III) at these temperatures.[47] The lifetime measurements of complex **3** indicate short lifetimes,

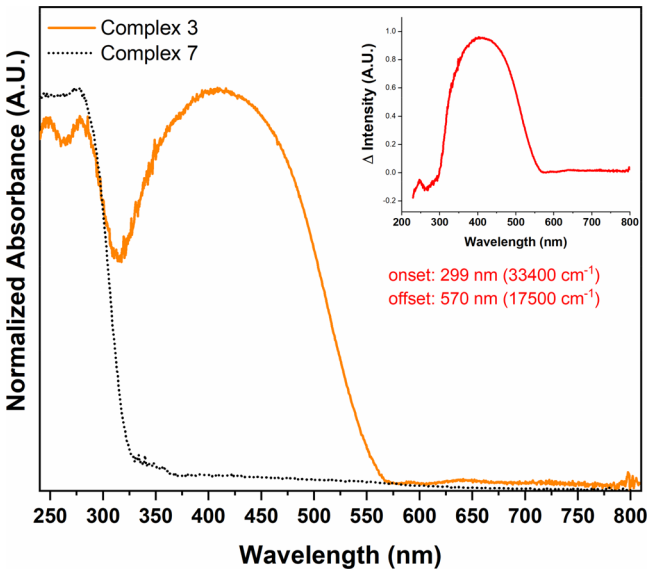

Figure 7. Normalized UV-vis absorbance spectra of $Eu[N(SPPh_2)_2]_3$ (**3**) and $Gd[N(SPPh_2)_2]_3$ (**7**) from 200 to 800 nm. Inset shows subtraction of the two spectra to determine LMCT energies.

~385 μs at 77K (shown in S12), further supporting the strong quenching of Eu(III) emitting states by the LMCT state. The lifetimes of the europium dithiocarbamate complexes were also lower than expected (<50 μs).[46]

The sensitivity of Eu(III) to LMCT quenching increases its interest as a luminescent molecular thermometer.[48] However, because the mechanism of thermal quenching increases with temperature, the emission of Eu(III) complexes typically becomes less intense as the temperature is increased to room temperature. This can be modified by identifying highly absorbing ligands with carefully tuned HOMO/LUMO energies, as reported by Hasegawa in $Eu(hfa)_3(DPCO)_2$ (hfa = hexaluforoacetylacetonate, and DPCO = diphenylphosphorylchrysene) which is quite intense at room temperature and quenches at 500 K.[48] Temperature-dependent Raman allowed us to monitor the emission of the $Eu[N(SPPh_2)_2]_3$ complex from 373 K down to 83 K (Figure 8). Based on the intensity of the $^5D_0-{}^7F_2$ transition as a function of temperature, the onset for quenching appears to be just above 130 K, so the emission range for this complex is limited to low temperatures. A comparison to the Gd analog (**7**) confirmed that the peaks were luminescence and not vibrations (S13).

Interestingly, we observed reversible orange (RT) to yellow (77 K) thermochromism of the $Eu[N(SPPh_2)_2]_3$ complex (**3**) (in S14 and S15). When heating above room temperature the color continues to shift to red. UV−visible diffuse reflectance measurements of the complex show a shift in the band edge as a function of temperature (S14). Several examples of thermochromic behavior have been observed in complexes with LMCT bands such as uranyl isothiocyanates, which exhibit similar red to yellow thermochromism.[49] In those systems, an interplay between the ratio of *intra-* to *inter*molecular charge transfer processes is important for understanding their thermochromic behaviors. In complex **3**, variable temperature single-crystal X-ray diffraction studies revealed a slight contraction in Eu−N bond lengths (shown in S16 and S17) with decreased temperature, as well as a contraction of the unit cell along the *a*- and *c*-axes. Analysis of

https://doi.org/10.1021/acs.inorgchem.2c02260
Inorg. Chem. 2022, 61, 15547−15557

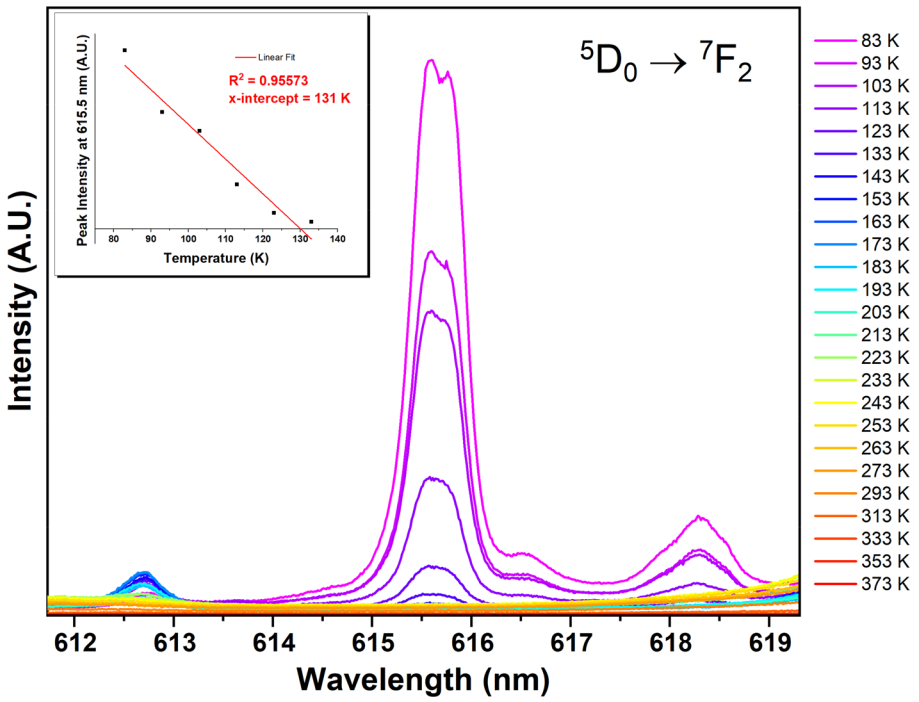

Figure 8. Variable temperature Raman spectra of $Eu[N(SPPh_2)_2]_3$ (**3**) showing Eu^{3+} luminescence growing in as temperature decreases. Inset shows a linear fit of peak intensity at 615.5 nm as a function of temperature, showing an onset luminescence temperature of ∼130 K.

the crystal structures in PLATON revealed no significant *inter*molecular interactions in both the 298 and 100 K structures, so we believe that the thermochromism exhibited in this complex is more *intra*molecular in nature (i.e., sensitive to the Eu−N bond distance). Further theoretical calculations are needed, however, to further investigate the mechanisms behind the thermochromism in this complex.

Luminescence of $Ln[S(QPPh_2)_2]_3$ Ln = Pr (4), Nd (5), Sm (6), Tb (8) and $Ln[Se(QPPh_2)_2]_3$ Ln = Pr (9), Nd (10), Sm (11). Room temperature luminescence was observed for the lanthanides, Pr, Nd, Sm, and Tb, as shown in Figure 9. The emissive properties of the lanthanides are often defined by two important processes, the absorption leading to population of the excited state and the extent to which nonradiative decay paths are deactivated.[1] Although direct excitation is possible, the oscillator strength of the f−f transitions is weak, leaving indirect excitation through the ligand as the most common method for excitation of lanthanides, which is referred to as the antenna effect. The first step of the antenna effect involves absorption of light by the ligand, leading to excitation of an excited singlet state, which is followed by intersystem crossing to a triplet state, and then intramolecular energy transfer to populate the emissive lanthanide ion level. One of the relevant questions is whether the dichalcogenoimidodiphosphinate ligand can sensitize lanthanides, and based on the excitation spectra of the complexes reported here, it is clearly possible.

The excitation and emission spectra for the sulfur and selenium analogs for Ln = Pr, Nd, Sm, and sulfur analog for Tb (the selenium complex did not crystallize) are shown in Figure 9. The emission intensities are quite similar for the sulfur and selenium analogs for each of these metals, suggesting little change in symmetry when S is replaced by Se. Because the energy gap between the lowest ligand triplet state is critical for effective transfer to the Ln(III) emitting level,[44] determining this energy is important. Given that the sulfur analog had a ^3T energy of 22 730 cm^{-1} and the selenium analog, 21 740 cm^{-1}, absent any nonradiative processes such as vibration-induced deactivation,[1] the triplet energies are appropriately positioned to undergo the energy transfer to the lanthanide 4f emissive states, as described for each metal.

Praseodymium is an interesting metal because it emits in both the visible and NIR regions of the spectrum (its emissive states are $^1I_6$ (21 000 cm^{-1}), $^3P_1$ (20 800 cm^{-1}), $^3P_0$ (20 050 cm^{-1}), and $^1D_2$ (16 500 cm^{-1})) and as a result can experience internal quenching. Thus, emission is primarily from $^3P_0$ and $^1D_2$,[50] and we observe only emission from the $^3P_0$, consistent with the proximity to the ligand triplet states. We do not see any evidence of NIR emission (two potential transitions $^1G_4 \rightarrow {}^3H_5$ at 1330 nm and $^1D_2 \rightarrow {}^1G_4$ at 1490 nm).[51] However, for neodymium we do observe strong emission in the NIR as expected for emission from the excited state $^4F_{3/2}$ (11 698 cm^{-1}). The excitation spectra of the Nd complexes are composed of broad ligand bands and narrow Nd(III) f−f intraconfigurational transitions (($^4D_{3/2}$, $_{5/2}$ + $^2I_{11/2}$) → $^4I_{9/2}$, ∼350 nm; ($^4G_{7/2}$, $_{9/2}$ + $^2K_{13/2}$) → $^4I_{9/2}$, ∼525 nm; and $^4G_{5/2}$, $_{7/2}$ → $^4I_{9/2}$, ∼580 nm) indicating that the direct excitation of the metal is competitive with the antenna effect. Upon excitation at the ligand bands (280 nm for complex **5** and 375 nm for complex **10**), the expected Nd(III)-centered $^4F_{3/2} \rightarrow {}^4I_J$ (J = 9/2, 11/2, and 13/2) transitions are present in the emission spectra and the $^4F_{3/2} \rightarrow {}^4I_{11/2}$ transition is the most intense one.

Samarium has three emissive excited states, $^4G_{7/2}$ (20 050 cm^{-1}), $^4F_{3/2}$ (18 700 cm^{-1}), and $^4G_{5/2}$ (∼17 700 cm^{-1}), and we only observe emission from the lowest energy excited state accessible by both ligands. Lifetime measurements of the samarium complexes (S9 and S10) show emission lifetimes that are comparable to similar soft-atom donor ligand systems such as the dithiocarbamates. $Sm[N(SPPh_2)_2]_3$ (**6**) exhibited a lifetime of 95.03 ± 0.35 μs, while the Se-analog (**11**) showed a lifetime of 50.39 ± 0.14 μs, both longer than that reported for

https://doi.org/10.1021/acs.inorgchem.2c02260
Inorg. Chem. 2022, 61, 15547−15557

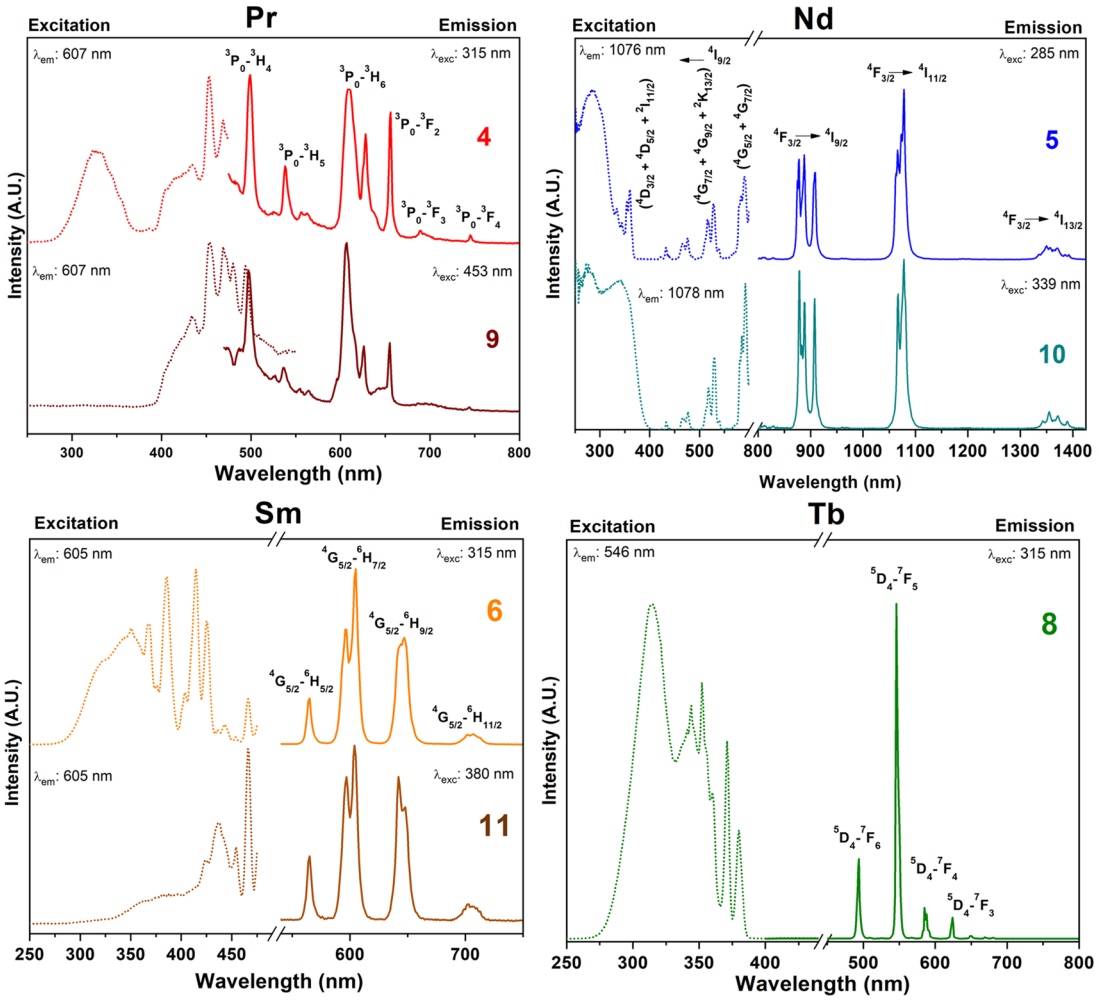

Figure 9. Room temperature (298 K) excitation and emission spectra of $Ln[N(QPPh_2)_2]_3$ Q = S (top), Se (bottom) for Ln = Pr (**4**, **9**), Ln = Nd (**5**, **10**), Ln = Sm (**6**, **11**), and Ln = Tb (**8**).

$Sm(S_2CNEt_2)_3phen$ (20.0 ± 0.1 μs).[26] Unfortunately, for terbium, we were only able to crystallize $Tb[N(SPPh_2)_2]_3$ (**8**), and emission was observed from the $^5D_4$ level (~20 500 cm^{-1}). Complex **8** showed emission lifetimes of ~1018 μs (S11).

CONCLUSION

The dichalcoimidodiphosphinate complexes provide a new example of lanthanide luminescence sensitization utilizing S- and Se-based ligands. The emission of the europium complexes was quite different for both trivalent and divalent complexes. The divalent complexes $Eu[N(SPPh_2)_2]_2(THF)_2$ (**1**) and $Eu[N(SePPh_2)_2]_2(THF)_2$ (**2**) highlight the significance of coordination environment distortions on the luminescent properties. The trivalent $Eu[N(SPPh_2)_2]_3$ (**3**) exhibits temperature-dependent luminescence which we ascribe to LMCT quenching at room temperature. In terms of tuning the emission spectra, we believe that the flexibility of the dichalcogenoimidodiphosphinate ligand offers a significant opportunity to investigate europium luminescence thermometry. It is a model system for determining the effects of symmetry (via tuning the denticity of the ligand), ligand donor ability (via electron donating or withdrawing nature of the R groups), and potentially the apical solvent molecules on Eu(II) luminescence.[52] The wide variability and functionality provided by this class of ligands allow for an easily tunable systems for europium luminescent thermometry.

Further experimental and theoretical studies utilizing structurally modified dichalcogenoimidodiphosphinate ligands are planned to help elucidate structure−property relationships on the thermochromic and temperature-sensitive luminescent behaviors of these complexes. In addition, studies using these complexes as single source precursors to nanomaterials is under investigation.

ASSOCIATED CONTENT

Supporting Information

The Supporting Information is available free of charge at https://pubs.acs.org/doi/10.1021/acs.inorgchem.2c02260.

Details of the synthesis and characterization of the complexes are provided in the Supporting Information. X-ray crystallographic files in CIF format for compounds $Eu[N(SPPh_2)_2]_2(THF)_2$ (**1**), $Pr[N(SPPh_2)_2]_3$ (**4**), $Nd[N(SPPh_2)_2]_3$ (**5**), $Sm[N(SPPh_2)_2]_3$ (**6**), $Eu[N(SPPh_2)_2]_3$ (**3**), $Gd[N(SPPh_2)_2]_3$ (**7**), $Tb[N(SPPh_2)_2]_3$ (**8**), $Pr[N(SePPh_2)_2]_3$ (**9**), $Sm[N(SePPh_2)_2]_3$ (**11**), $Gd[N(SePPh_2)_2]_3$ (**12**) and were deposited in the Cambridge Structure Database with CCDC numbers 2172679 (**1**), 2172677 (**1** @ 298 K), 2172678 (**2** @ 298 K), 2172666 (**3**), 2172676 (**3** @ 298 K), 2172673 (**4**),

https://doi.org/10.1021/acs.inorgchem.2c02260
Inorg. Chem. 2022, 61, 15547−15557

2172672 (**5**), 2172668 (**6**), 2172674 (**7**), 2172670 (**8**), 2172675 (**9**), 2172667 (**11**), 2172671 (**12**). (PDF)

Accession Codes

CCDC 2172666−2172679 contain the supplementary crystallographic data for this paper. These data can be obtained free of charge via www.ccdc.cam.ac.uk/data_request/cif, or by emailing data_request@ccdc.cam.ac.uk, or by contacting The Cambridge Crystallographic Data Centre, 12 Union Road, Cambridge CB2 1EZ, UK; fax: +44 1223 336033.

AUTHOR INFORMATION

Corresponding Author

Sarah L. Stoll − *Department of Chemistry, Georgetown University, Washington, D.C. 20057, United States;* orcid.org/0000-0001-7184-8672; Email: sls55@georgetown.edu

Authors

Orlando C. Stewart, Jr. − *Department of Chemistry, Georgetown University, Washington, D.C. 20057, United States*

Alexander C. Marwitz − *Department of Chemistry, Georgetown University, Washington, D.C. 20057, United States;* orcid.org/0000-0002-2560-9184

Joel Swanson − *Department of Chemistry, Georgetown University, Washington, D.C. 20057, United States*

Jeffery A. Bertke − *Department of Chemistry, Georgetown University, Washington, D.C. 20057, United States;* orcid.org/0000-0002-3419-5163

Tyler Hartman − *Department of Chemistry, Georgetown University, Washington, D.C. 20057, United States;* orcid.org/0000-0002-1897-8782

Jorge H. S. K. Monteiro − *Department of Chemistry, California Polytechnic State University, Humboldt, Arcata, California 95521, United States;* orcid.org/0000-0002-9622-3537

Ana de Bettencourt-Dias − *Department of Chemistry, University of Nevada, Reno, Reno, Nevada 89557, United States;* orcid.org/0000-0001-5162-2393

Karah E. Knope − *Department of Chemistry, Georgetown University, Washington, D.C. 20057, United States;* orcid.org/0000-0002-5690-715X

Complete contact information is available at: https://pubs.acs.org/10.1021/acs.inorgchem.2c02260

Funding

NSF (CHE-1904616) SLS NSF (CHE-1800392) to A.d.B.D., Orlando Stewart acknowledges the Healy Fellowship that supported this work.

Notes

The authors declare no competing financial interest.

ACKNOWLEDGMENTS

We thank the National Science Foundation for funding this work (CHE-1904616), and CHE-1800392 to A.d.B.D.

REFERENCES

(1) Bunzli, J. C.; Piguet, C. Taking advantage of luminescent lanthanide ions. *Chem. Soc. Reviews* **2005**, *34*, 1048−1077.

(2) Dorenbos, P. Energy of the first 4f7−>4f65d transition of Eu^{2+} in inorganic compounds. *J. Lumin.* **2003**, *104* (4), 239−260.

(3) Murray, G.; Sarrio, R.; Peterson, J. Correlation of Raman Phonon and Europium(Ill) LuminescenceSpectra as a Probe of Structure in Trisodium Tris(2,6-pyridinedicarboxylato)lanthanide-(III) Compounds. *Appl. Spectrosc.* **1990**, *44* (10), 1647−1653.

(4) Monteiro, J.; Sigoli, F.; de Bettencourt-Dias, A. A water-soluble TbIII complex as a temperature-sensitive luminescent probe. *Can. J. Chem.* **2018**, *96*, 859−864.

(5) Yanagisawa, K.; Kitagawa, Y.; Nakanishi, T.; Seki, T.; Fushimi, K.; Ito, H.; Hasegawa, Y. A Luminescent Dinuclear EuIII/TbIII complex with LMCT Band as a Single-Molecular Thermosensor. *Chem.—Eur. J.* **2018**, *24*, 1956−1961.

(6) Kitagawa, Y.; Ferreira da Rosa, P.; Hasegawa, Y. Charge-transfer excited states of π- and 4f-orbitals for development of luminescent. *Dalton Trans.* **2021**, *50*, 14978−14984.

(7) Diaz-Rodriguez, R.; Galico, D.; Chartrand, D.; Suturina, E.; Murugesu, M. Toward Opto-Structural Correlation to Investigate Luminescence Thermometry in an Organometallic Eu(II) Complex. *J. Am. Chem. Soc.* **2022**, *144*, 912−921.

(8) Regulacio, M. D.; Kar, S.; Zuniga, E.; Wang, G.; Dollahon, N. R.; Yee, G. T.; Stoll, S. L. Size-Dependent Magnetism of EuS Nanoparticles. *Chem. Mater.* **2008**, *20* (10), 3368−3376.

(9) Atif, R.; Zarkov, A.; Asuigui, D. R. C.; Glaser, P.; Stewart, O.; Stoll, S. Single Source Precursors for Lanthanide Diselenide Nanosheets. *Chem. Mater.* **2019**, *31*, 7779−7789.

(10) Schmidpeter, A.; Bohm, C. R.; Groeger, H. Imidodiphosphinatometal Chelates Neutral Complexes with carbon-free chelate rings. *Angew. Chem., Int. Ed.* **1964**, *3*, 704.

(11) Bhattacharyya, P.; Slawin, A.; Williams, D.; Woollins, D. Preparation and Characterisation of [Pt{N(SePPh2)2-Se,Se'}$(PR_2)_2$]Cl(R = alkyl or aryl); Crystal Structure of [Pd{Ph_2PNP(Se)Ph_2-P,Se}{N($SePPh_2$)$_2$-Se,Se'}]$_{0.5}EtOH_{0.3}CH_2Cl_2$. *J. Chem. Soc., Dalton Trans.* **1995**, 2489−2495.

(12) Chivers, T.; Eisler, D.; Ritch, J.; Tuononen, H. An Unusual Ditelluride: Synthesis and Molecular and Electronic Structures of the Dimer of the Tellurium-Centered Radical [$TePiPr_2NiPr_2PTe$]. *Angew. Chem., Int. Ed.* **2005**, *44*, 4953−4956.

(13) Copsey, M.; Panneerselvam, A.; Afzaal, M.; Chivers, T.; O'Brien, P. Syntheses, X-ray structures and AACVD studies of group 11 ditelluroimidodiphosphinate complexes. *Dalton Trans.* **2007**, 1528−1538.

(14) Panneerselvam, A.; Periyasamy, G.; Ramasamy, K.; Afzaal, M.; Malik, M.; O'Brien, P.; Burton, N.; Waters, J.; van Dongen, B. Factors controlling material deposition in the CVD of nickel sulfides, selenides or phosphides from dichalcogenoimidodiphosphinato complexes: deposition, spectroscopic and computational studies. *Dalton Transactions* **2010**, *39*, 6080−6091.

(15) Oyetunde, T.; Afzaal, M.; O'Brien, P. Phenyl substituted ditelluro-imidodiphosphinate complexes of iron, nickel, palladium and platinum, and their pyrolysis studies generating metal tellurides. *Polyhedron* **2019**, *160*, 157−162.

(16) Afzaal, M.; Malik, M.; O'Brien, P. Chemical routes to chalcogenide materials as thin films or particles with critical dimensions with the order of nanometres. *J. Mater. Chem.* **2010**, *20*, 4031−4040.

(17) Akhtar, M.; Malik, M. A.; Raftery, J.; O'Brien, P. Synthesis of iron selenide nanocrystals and thin films from bis-(tetraisopropyldiselenoimidodiphosphinato)iron(ii) and bis-(tetraphenyldiselenoimidodiphosphinato)iron(ii) complexes. *Journal of Materials Chemistry A* **2014**, *2*, 20612−20620.

(18) Gaunt, A. J.; Scott, B. L.; Neu, M. P. Homoleptic uranium(III) imidodiphosphinochalcogenides including he first structurally characterised molecular trivalent actinide-Se Bond. *Chem. Commun.* **2005**, No. 25, 3215−3217.

(19) Goodwin, C. A. P.; Schlimgen, A. W.; Albrecht-Schönzart, T. E.; Batista, E. R.; Gaunt, A. J.; Janicke, M. T.; Kozimor, S. A.; Scott, B. L.; Stevens, L. M.; White, F. D.; Yang, P. Structural and Spectroscopic Comparison of Soft-Se vs. Hard-O Donor Bonding in Trivalent Americium/Neodymium Molecules. *Angew. Chem.* **2021**, *60*, 9459−9466.

(20) Jensen, M.; Bond, A. Comparison of Covalnecy in the Complexes of Trivalent Actinide and Lanthanide Cations. *J. Am. Chem. Soc.* **2002**, *124*, 9870−9877.
(21) Magennis, S. W.; Parsons, S.; Corval, A.; Woollins, J. D.; Pikramenou, Z. Imidodiphosphinate ligands as antenna units in luminescent lanthanide complexes. *Chem. Commun.* **1999**, No. 1, 61−62.
(22) Magennis, S.; Parsons, S.; Pikramenou, Z. Assembly of Hydrophobic Shells and Shields around Lantahnides. *Chem.—Eur. J.* **2002**, *8* (24), 5761−5771.
(23) Li, S. J.; Li, K. A novel photo and thermal stable dysprosium complex with tetraphenylimidodiphosphinate acid. *Russ. J. Coord. Chem. Khimiya* **2014**, *40* (3), 189−193.
(24) Davis, D.; Carrod, A. J.; Guo, Z.; Kariuki, B. M.; Zhang, Y. Z.; Pikramenou, Z. Imidodiphosphonate Ligands for Enhanced Sensitization and Shielding of Visible and Near-Infrared Lanthanides. *Inorg. Chem.* **2019**, *58* (19), 13268−13275.
(25) Bassett, A. P.; Van Deun, R.; Nockemann, P.; Glover, P. B.; Kariuki, B. M.; Van Hecke, K.; Van Meervelt, L.; Pikramenou, Z. Long-Lived Near-Infrared Luminescent Lanthanide Complexes of Imidodiphosphinate "Shell" Ligands. *Inorg. Chem.* **2005**, *44* (18), 6140−6142.
(26) Regulacio, M. D.; Pablico, M. H.; Vasquez, J. A.; Myers, P. N.; Gentry, S.; Prushan, M.; Tam-Chang, S.-W.; Stoll, S. L. Luminescence of Ln(III) Dithiocarbamate Complexes (Ln = La, Pr, Sm, Eu, Gd, Tb, Dy). *Inorg. Chem.* **2008**, *47* (5), 1512−1523.
(27) Pushkarev, A.; Yablonskiy, A.; Yunin, P.; Burin, M. E.; Andreev, B.; Bochkarev, M. Features of spectral properties of Sm3 + complexes with dithia- and diselenophosphinate ligands. *Spectrochimica Acta Part A Molecular and Biomolecular Spectroscopy* **2016**, *163*, 134−139.
(28) Bryleva, Y.; Kokina, T. E.; Glinskaya, L. A.; Rakhmanova, M. I.; Kurateva, N. V.; KorolKov, I. V.; Larionov, S. V. Synthesis and photoluminescence of complexes Tm(L)(iso-Bu_2PS_2)$_2$(NO_3) (L = Phen, 2,2′-Bipy). Crystal structures of compounds [Ln(2,2′-Bipy)-(iso-Bu_2PS_2 $_2$(NO_3)·C_6H_6 (Ln = Tm, Tb). *Russian Journal of Coordination Chemistry* **2013**, *39* (10), 738−745.
(29) Bryleva, Y. A.; Artem'ev, A. V.; Glinskaya, L. A.; Komarov, V. Y.; Bogomyakov, A. S.; Rakhmanova, M. I.; Larionov, S. V. A series of bis(2-phenethyl)dithiophosphinate-based Ln(III) complexes: Synthesis, magnetic and photoluminescent properties. *Inorg. Chim. Acta* **2021**, *516*, 120097.
(30) Zheng, Y.; Zhou, L.; Lin, J.; Zhang, S. Syntheses and Crystal Structures of Ln(phen)$_2$(NO_3)$_3$ with Ln = Pr, Nd, Sm, Eu, Dy, and phen = 1,10-phenanthroline. *Zeitschrift für Anorg. und Allg. Chemie* **2001**, *627* (7), 1643−1646.
(31) Goodwin, C.; Janicke, M.; Scott, B.; Gaunt, A. [$AnI_3(THF)_4$] (an = Np, Pu) Preparation Bypassing An^0 Metal Precursors: Access to Np^{3+}/Pu^{3+} Nonaqueous and Organometallic Complexes. *J. Am. Chem. Soc.* **2021**, *143*, 20680−20696.
(32) Geissinger, M.; Magull, J. Synthesis and Reactivity of Samarium Complexes with Bis (diphenylchalcogenophosphoryl) amides. The Structures of [{η^2-(Ph_2PS)$_2$N}$_2$Sm(thf)$_2$], [{η^3(Ph_2PSe)ZN}-{η^2(Ph_2PSe) $_2$N}Sm(thf)], [{η^3(Ph_2PSe) $_2$N}$_2$Sm(SePh)(thf), and [{η^3(Ph_2PSe)$_2$N}Sm(SeMes)(thf)]. *Z. anorg. allg. Chem.* **1997**, *623*, 755−761.
(33) Ingram, K.; Kaltsoyannis, N.; Gaunt, A.; Neu, M. Covalency in the f-element−chalcogen bond Computational studies of [M(N-(EPH_2)$_2$)$_3$] (M = La, U, Pu;E = O,S,Se, Te). *J. Alloys Compd.* **2007**, *444*−*445*, 369−375.
(34) Garcia, J.; Allen, M. Developments in the Coordination Chemistry of Europium (II). *Eur. J. Inorg. Chem.* **2012**, *2012*, 4550−4563.
(35) Regulacio, M. D.; Tomson, N.; Stoll, S. L. Dithiocarbamate Precursors for Rare-Earth Sulfides. *Chem. Mater.* **2005**, *17* (12), 3114−3121.
(36) Davis, D.; Carrod, A.; Guo, Z.; Kariuki, B.; Zhang, Y.; Pikramenou, Z. Imidodiphosphonate Ligands for Enhanced Sensitization and Shielding of Visible and Near-Infrared Lanthanides. *Inorg. Chem.* **2019**, *58*, 13268−13275.
(37) Heitmann, D.; Jones, C.; Junk, P.; Lippert, K.; Stasch, A. Homoleptic lanthanide(ii)−bis(guanidinate) complexes, [Ln(Giso)$_2$] (Giso = [$(ArN)_2CN(C_6H_{11})_2$]−, Ar = $C_6H_3Pri_2$-2,6): planar 4-coordinate (Ln = Sm or Eu) vs distorted tetrahedral (Ln = Yb) geometries. *Dalton Trans.* **2007**, 187−189.
(38) Heitmann, D.; Jones, C.; Mills, D.; Stasch, A. Low coordinate lanthanide(II) complexes supported by bulky guanidinato and amidinato ligands. *Dalton Trans.* **2010**, *39*, 1877−1882.
(39) Gaunt, A.; Reilly, S.; Enriquez, A.; Scott, B.; Ibers, J.; Sekar, P.; Ingram, K.; Kaltsoyannis, N.; Neu, M. Experimental and Theoretical Comparison of Actinide and Lanthanide Bonding in M[$N(EPR_2)_2$]$_3$ Complexes (M = U, Pu, La, Ce; E = S, Se, Te; R = Ph, iPr, H). *Inorg. Chem.* **2008**, *47* (1), 29−41.
(40) Shavaleev, N.; Eliseeva, S.; Scopelliti, R.; Bunzli, J. C. Influence of Symmetry on the Luminescence and Radiative Lifetime of Nine-Coordinate Europium Complexes. *Inorg. Chem.* **2015**, *54*, 9166−9173.
(41) Gaunt, A.; Scott, B.; Neu, M. A Molecular Actinide−Tellurium Bond and Comparison of Bonding in [MIII{$N(TePiPr_2)_2$}$_3$] (M = U, La). *Angew. Chem., Int. Ed.* **2006**, *45*, 1638−1641.
(42) Gaunt, A. J.; Scott, B.; Neu, M. Homoleptic uranium(III) imidodiphosphinochalcogenides including the first structurally characterized molecular trivalent actinide-Se bond. *Chem. Commun.* **2005**, 3215−3217.
(43) Dorenbos, P. Anomalous Luminescence of Eu^{2+} and Yb^{2+} in Inorganic Compounds. *J. Phys.: Condens. Matter* **2003**, *15*, 2645−2665.
(44) Latva, M.; Takalo, H.; Mukkala, V.; Matachescu, C.; Rodriguez-Ubis, J.; Kankare, J. Correlation between the lowest triplet state energy level of the ligand and lanthanide(III) luminescence quantum yield. *J. Lumin.* **1997**, *75*, 149−169.
(45) Bünzli, J.-C. G. On the design of highly luminescent lanthanide complexes. *Coord. Chem. Rev.* **2015**, *293*−*294*, 19−47.
(46) Faustino, W.; Malta, O.; Teotonio, E.; Brito, H.; Simas, A.; de Sa, G. Photoluminescence of europium(III) dithiocarbamate complexes: Electronic structure, charge transfer and energy transfer. *J. Phys. Chem. A* **2006**, *110*, 2510−2516.
(47) Gálico, D. A.; Souza, E. R.; Mazali, I. O.; Sigoli, F. A. High relative thermal sensitivity of luminescent molecular thermometer based on dinuclear [$Eu_2(mba)_4(\mu$-$mba)_2(H_2O)_2$] complex: The role of inefficient intersystem crossing and LMCT. *J. Lumin.* **2019**, *210*, 397−403.
(48) Kitagawa, Y.; Kumagai, M.; Nakanishi, T.; Fushimi, K.; Hasegawa, Y. The Role of π−f Orbital Interactions in Eu(III) Complexes for an Effective Molecular Luminescent Thermometer. *Inorg. Chem.* **2020**, *59*, 5865−5871.
(49) Surbella, R. G.; Ducati, L. C.; Autschbach, J.; Deifel, N. P.; Cahill, C. L. Thermochromic Uranyl Isothiocyanates: Influencing Charge Transfer Bands with Supramolecular Structure. *Inorg. Chem.* **2018**, *57* (5), 2455−2471.
(50) Voloshin, A.; Shavaleev, N.; Kazakov, V. Luminescence of praseodymium (III) chelates from two excited states (3P0 and 1D2) and its dependence on ligand triplet state energy. *J. Lumin.* **2001**, *93*, 199−204.
(51) Zhou, B.; Pun, Y.-B. Super broadband near-IR emission from praseodymium-doped bismuth gallate glasses. *Opt. Lett.* **2011**, *36* (15), 2958−2960.
(52) Galimov, D. I.; Yakupova, S. M.; Vasilyuk, K. S.; Sabirov, D. S.; Bulgakov, R. G. Effect of coordination environment of Eu^{2+} ion on the 5d-4f luminescence of molecular compounds $EuL_2(THF)_x$ (L = Cl, Br, I, NO_3, Ac, fod, tmhd, and acac; x = 0, 2). *Journal of Photochemistry & Photobiology, A: Chemistry* **2020**, *403*, 112839.

https://doi.org/10.1021/acs.inorgchem.2c02260
Inorg. Chem. 2022, 61, 15547−15557